Electron capture decay of indium-111 human carbonic anhydrase I: A time differential K X ray coincidence perturbed angular correlation study

Christopher Haydock*
Research Computing Facility
Mayo Foundation, Rochester, MN, USA

The relaxation effects in the perturbed angular correlation spectra of ^{111}In human carbonic anhydrase I (HCA I) are the result of chemical transmutation and/or the complex Auger cascades that follow the electron capture decay of ^{111}In. Time differential K X ray coincidence perturbed angular correlation (PAC) spectroscopy shows that these relaxation effects are independent of the Auger cascade intensity. This suggests that chemical transmutation is responsible for the relaxation effects, and that bond breaking and damage product formation around the decay site resulting from localized energy deposition by Auger and Coster-Kronig electrons probably occur in the microsecond time regime. Numerical simulations of chemical transmutation relaxation effects in the time differential PAC spectrum of ^{111}In HCA I are also presented.

Introduction

Perturbed angular correlation spectroscopy (PAC) is a potential technique for investigating hot atom chemistry following electron capture decay of a radionuclide probe [1, 2]. As is the case with Mössbauer emission spectroscopy, it may be possible to identify the chemical form of the probe nuclide coordination complex during the nuclear lifetime [3, 4]. The average Auger and Coster-Kronig electron yield is significantly diminished when the vacancy cascade following electron capture includes the emission of a K X ray as compared to when it does not. It is in principle possible to study the dependence of hot atom chemistry on the intensity of Auger and Coster-Kronig emissions by detecting the nuclear radiations of perturbed angular correlation or Mössbauer emission spectroscopy in coincidence with K shell X rays [5, 6]. Given the very limited knowledge of hot atom chemistry of electron capture nuclides that are possible perturbed angular correlation probes, one may ask only a yes or no question. Does or does not the hot atom chemistry depend electron emission intensity? To answer this, a chemical transmutation model and a dose dependent damage model are constructed for the perturbed angular correlation spectra following electron capture. Both models encompass several alternative pictures of the hot atom chemistry. The simplest hot atom chemistry of the chemical transmutation model is very similar to β^+ decay on the nanosecond time scale. Note that β^+ decay is energetically forbidden for ^{111}In. The multiple Auger ionization processes are followed by complete electron recombination that leaves the daughter nuclide in a metastable state with both the atomic number and valence decreased by one unit from the parent. The metastable state is the result of the change in charge rather that charge neutralization or Auger electron irradiation. The metastable state of the daughter nuclide decays within tens of nanoseconds to the ground state coordination complex of the daughter and ligands. However, any hot atom chemistry involving an excited state of the daughter that decays thereafter into the ground state complex is equally consistent with the chemical transmutation model. The only requirement is that the excited state be independent of Auger emission intensity. The dose dependent damage model pictures radiolytic fragmentation of probe coordination complex ligands. The amplitudes and rates of ligand fluctuations increase with the intensity of the Auger emissions. Though uncertain about the details of hot atom chemistry both models predict perturbed angular correlation spectra. The comparison of these spectra with experimental data indicates whether or not the hot atom chemistry during the nanoseconds following electron capture depends on Auger emission intensity.

A partial decay scheme for ^{111}In and ^{111m}Cd is shown in Fig. 1. Perturbed angular correlation spectra of the isomeric ^{111m}Cd decay provide the quadrupole interaction parameters of the ground state coordination complex in the chemical transmutation model and the ligand relaxation parameters at zero dose in the dose dependent damage model. Following ^{111}In electron capture decay the ^{111}Cd daughter is in a 120 picosecond nuclear excited state that initiates the 171–245 keV gamma cascade. Processes occurring faster than the lifetime of this initial nuclear state, including dissipation of thermal hot spots [3, 8], do not influence perturbed angular correlation spectra. The spectra reflect the hot atom chemistry occurring during the lifetime of the intermediate state. Indirect effects involving the diffusion of water radicals are not observed. A great variety of radiochemical and radiobiological experiments show that direct and indirect processes together result in damage that is proportional to the Auger emission intensity. For example, when zinc bovine carbonic anhydrase is X ray irradiated just above

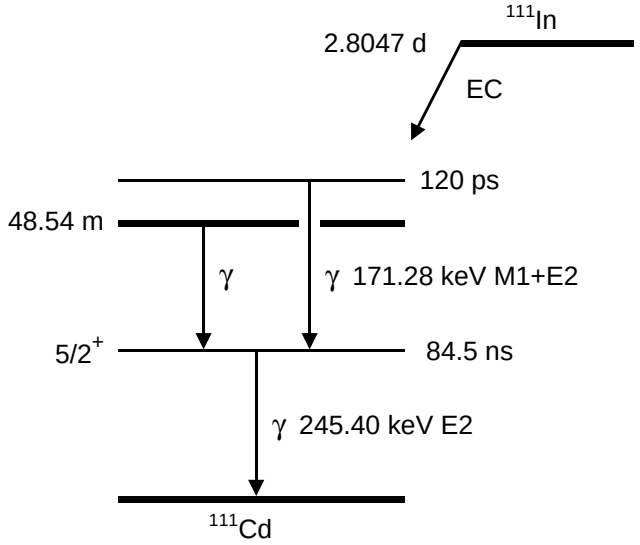

FIG. 1: Partial decay scheme for ^{111}In and ^{111m}Cd [7]. The half-life of each level is labeled. The 171–245 keV gamma cascade follows the electron capture decay of ^{111}In; the 48.5 minute ^{111m}Cd state decays by the 151–245 keV gamma cascade. Both cascades share the same 245 keV 5/2+ ^{111}Cd intermediate nuclear state.

the zinc K edge, enzyme activity and zinc release assays indicate significant Auger inactivation [9]. The more intense Auger emissions accompanying ^{111}In decay can be expected to inactivate HCA I even more effectively. The combined direct and indirect effects are Auger emission intensity dependent. An Auger dependent effect on the nanosecond time scale can be detected with K X ray coincidence perturbed angular correlation spectroscopy.

Materials and Methods

Human carbonic anhydrase I was isolated from freshly outdated erythrocytes [10]. The apoenzyme was obtained by dialysis at 4°C against pyridine-2,6-dicarboxylic acid [11]. HCA I activity was assayed spectrophotometrically with *p*-nitrophenyl acetate (Sigma Chemical Co., St. Louis, Missouri) as substrate [12]. Conventional time differential gamma-gamma perturbed angular correlation spectra of ^{111}In labeled HCA I were measured on a movable two detector perturbed angular correlation spectrometer [13]. A 2 by 2 inch cylindrical BC-404 plastic scintillator with 0.25 inch centered side bore for internal sample mounting and RCA 8575 phototube detected the K X rays. Coincidence gating electronics, including a time to pulse height converter for coincidence timing K X rays and the gamma-gamma cascade, selected either K X ray coincidence or anti-coincidence spectra for storage and analysis. Carrier free ^{111}In in 0.05 molar HCl (Du Pont de Nemours & Co. Inc., Wilmington, Delaware) was ordered at two week intervals. Apo-HCA I was incubated for 48 h with ^{111}In in 100 mM HEPES buffer (Research Organics Inc., Cleveland, Ohio) at pH 7.7 with sodium citrate acting as carrier for indium. In order to hold constant both the volume and total indium concentration, the specific activity of the ^{111}In stock was adjusted with cold indium chloride. After labeling with indium, the effects of HCA I rotational motions on the perturbed angular correlation spectrum were diminished by adding sucrose to a final concentration by weight of 50%. Seven labeled protein samples were prepared from each shipment of ^{111}In. A perturbed angular correlation spectrum was accumulated for 46 h from each sample. The first and last samples were run as incubation controls. These samples were measured for an initial twelve h as ^{111}In-citrate; HCA I was added, and the measurement was continued for another 34 h. The time integral perturbation factors accumulated for 20 min intervals monitored the HCA I labeling reaction. All spectra from shipments that did not give excellent labeling were discarded. Three of the five non-control samples per shipment were measured in K X ray coincidence mode and two in K X ray anti-coincidence mode. A total of 52 coincidence mode samples and 36 anti-coincidence mode samples were combined for analysis. All sample preparations and measurements were done at 21 ± 1°C.

Electron capture gamma-gamma perturbed angular correlation spectra measure the ensemble average electric quadrupole relaxation of the daughter nucleus spin. Magnetic dipole interactions are assumed to be negligible. The measurable parameters are model dependent. All models must contain one or more rate constants that characterize the time dependence of the quadrupole interactions. In the chemical transmutation model, spin relaxation is the result of the decay of a metastable state of the daughter nucleus coordination complex. This metastable state might be a valence electron, coordination geometry, or ligand conformation state. In any case, the quadrupole interaction parameters of the initial metastable state are the frequency mean, frequency standard deviation, asymmetry, and the mean lifetime of the state. The initial state decays into the ground state coordination complex. The interaction parameters of the ground state are the frequency mean, frequency standard deviation, asymmetry, and Euler rotation angles relative to the initial state. The initial and ground state interaction frequencies are independent Gaussian distributions. Each individual daughter nucleus interacts with the initial and ground state coordination complexes at fixed quadrupole frequencies that are randomly and independently sampled from the respective Gaussian distributions. The lifetimes of the initial interactions are given by an exponential distribution. In addition to relaxation from coordination complex decay, the chemical transmutation model includes relaxation from overall molecular tumbling by multiplying the spectrum with an exponential factor.

The dose dependent damage model ascribes the spin relaxation to ligand reorientation in the coordination complex. The quadrupole interaction parameters of the coordination complex are the mean frequency, frequency standard deviation, asymmetry, rotation angle standard deviation, and jump rate. These five parameters depend linearly on dose to the coordination complex and have a baseline value for the zero dose coordination complex. The electric field gradient orientation distribution is defined by rotations from a reference orientation, where the rotation angle distribution is Gaussian and the rotation axis distribution is isotropic. Note that though there is a single reference orientation in this interaction model, the perturbed angular correlation spectrum is for an isotropic source because the interactions of each daughter nucleus are averaged over random orientations when the spectrum is computed. The interaction frequency distribution is a Gaussian. Both the interaction frequency and orientation are sampled after every jump. The time intervals between jumps are exponentially distributed.

In both the chemical transmutation and dose dependent damage models, the interaction of each individual daughter nucleus is piecewise static and each set of model parameters specifies a probability distribution function for piecewise static interactions. The perturbation factor (which is loosely refered to as the perturbed angular correlation spectrum), is the average over this probability distribution of the perturbation factor of each piecewise static interaction. For a piecewise static interaction averaged over random source orientations, the perturbation factors are [13],

$$\begin{aligned} G_{kk}(t) &= \sum_{m_a m_b N} \Big\{ (-1)^{2I+m_a+m_b} \\ &\quad \times \begin{pmatrix} I & I & k \\ m'_a & -m_a & N \end{pmatrix} \begin{pmatrix} I & I & k \\ m'_b & -m_b & N \end{pmatrix} \\ &\quad \times \langle m_b|\Lambda(t)|m_a\rangle \langle m'_b|\Lambda(t)|m'_a\rangle^* \Big\}, \end{aligned} \tag{1}$$

where k is an even index, t is the delay time between emission of the two gamma rays from the daughter nucleus gamma-gamma cascade, I is the spin of the intermediate nuclear state, m_a, m'_a, m_b, and m'_b index magnetic substates of the intermediate state, the matrix element coefficients are the Wigner 3-j symbols, and $\Lambda(t)$ is the piecewise static time evolution operator. Since only $G_{22}(t)$ is usually measurable, it is refered to as the perturbation factor. The index N takes all integer values with absolute value less than or equal to k and the primed magnetic substate indices are given by $m'_a - m_a + N = 0$ and $m'_b - m_b + N = 0$. Since the perturbation factor is always computed at a series of time points, it is appropriate to express the piecewise static time evolution operator as a series operator product of interval evolution operators. The interval evolution operator for the time interval (t', t) is a series operator product of static evolution operators,

$$\Lambda(t', t) = \prod_{j=J'}^{J} e^{-iH_j t_j/\hbar}, \tag{2}$$

where H_j is the j^{th} time independent interaction Hamiltonian, J is the index of the first Hamiltonian with active interval overlapping (t', t), J' is the index of the last Hamiltonian with active interval overlapping (t', t), and t_j is the time overlap of (t', t) and the active time interval of the j^{th} Hamiltonian. Matthias et al. [14] give the electric quadrupole Hamiltonian matrix elements for arbitrary intermediate spin, interaction frequency, asymmetry parameter, and y convention [15] orientation. The quadrupole interaction frequency is specified by the angular frequency ω_0. By definition, ω_0 equals 3 times the quadrupole interaction frequency for integer spin and 6 times the quadrupole interaction frequency for half integer spin. When the electric quadrupole Hamiltonian is axially symmetric $\omega_0\hbar$ equals the smallest nonvanishing eigenvalue difference. The angular frequency ω_0 is frequently reported with correct numerical value but with the erroneous dimension of Hertz [16].

The piecewise static perturbation factors were evaluated by repeated extension of the time evolution operators in increments of $0.025(2\pi/\omega_0)$, where ω_0 was the mean angular frequency of the ground state or zero dose coordination complex. The evolution operator at each time point was extended to the next time point by matrix multiplication with a time interval evolution operator. Each time interval evolution operator was a product of static evolution operators with the Hamiltonian indices and overlap intervals indicated in Eq. (2). The interaction Hamiltonians were diagonalized [17]; the static evolution operators were expressed in diagonal form with the eigenvalues, transformed back into the magnetic substate representation with the eigenvectors, and multiplied together to give the time interval evolution operators. Since in the parameter domain of interest the perturbation factor time intervals were an order of magnitude smaller than the typical static Hamiltonian active time interval, most interval evolution operators were a single static evolution operator and each Hamiltonian diagonalization generated many interval evolution operators. The time interval evolution operators were repeatedly multiplied to give the evolution operators at a series of 160 time points. The matrix elements of the evolution operators were inserted in Eq. (1) to give the piecewise static perturbation factors at these time points.

The piecewise static perturbation factor probability distribution function was averaged by Monte Carlo integration [18]. Perturbation factor error estimates were calculated from the deviation of subaverages around the overall average as a function of the spectrum delay time. Gaussian interaction frequency and rotation angle distributions were generated by summing uniform random

variates. Excited state and orientation lifetimes were generated by logarithmic transform of uniform random numbers on the unit interval. Isotropic rotation directions were generated by an acceptance-rejection technique [19]. Random numbers uniform on the unit interval were generated by a 32-bit linear congruential pseudo-random generator with divisor $2^{31}-1$ and multiplier 7^5.

Initially the qualitative dependence of the perturbation factor on parameter space of the chemical transmutation and the dose dependent damage models was coarsely surveyed. The chemical transmutation model metastable state lifetime, ground state rotation angle, and relative magnitude of the metastable and ground state mean interaction frequency parameters were varied. Based on the preliminary survey and known ground state coordination complex parameters, a crude estimate was made of the parameter point that fit the data. This fit was refined by varying the unknown parameters one at a time until the residuals were about the same magnitude as the experimental error. The chemical transmutation model ground state frequency mean, frequency standard deviation, and asymmetry and the overall tumbling relaxation time constant were fixed at the known values. The Euler rotation angles relative to the initial state were fixed at values found in the preliminary survey to give strong spin relaxation. The initial metastable state was assumed to be axially symmetric, and the frequency mean and frequency standard deviation were varied.

The preliminary dose dependent damage model parameter survey fixed the mean frequency, frequency standard deviation, and asymmetry parameters at the known zero dose coordination complex values, and varied the rotation angle standard deviation and jump rate parameters. By comparing of the results of this search and the perturbation factor measured by Bauer et al. [20] with the assumption that spin relaxation is due to molecular tumbling, values were identified for the rotation angle standard deviation and jump rate parameters approximately equivalent to the molecular tumbling time constant of the zero dose coordination complex. The preliminary search also yielded the initial parameter point for fitting the dose dependent damage model to the data. The mean frequency, frequency standard deviation, asymmetry, rotation angle standard deviation, and jump rate parameters were all varied.

During the preliminary parameter space searches and parameter refinement, the perturbation factors were computed by averaging 10^3 piecewise static interactions. The standard deviations of these perturbation factors were fairly independent of spectrum delay time and typically about 0.01. The displayed perturbation factors were averaged over 10^4 interactions to give a standard deviation of about 0.003. All calculations were done on a DEC VAX 3600 or Silicon Graphics 4D workstation.

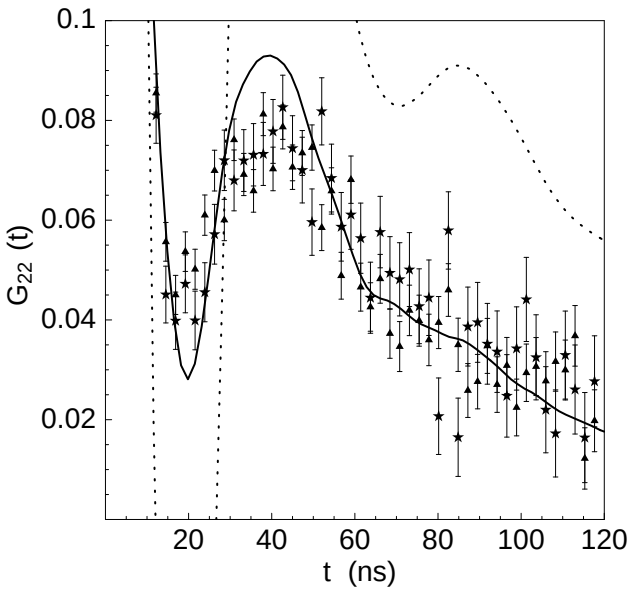

FIG. 2: Chemical transmutation model for HCA I perturbed angular correlation spectra. The triangles with standard error markers are the K X ray anti-coincidence spectrum and the stars with standard error markers are the K X ray coincidence spectrum. The solid curve is an approximate fit of the chemical transmutation model to the data. The dotted curve is the least squares fit of Bauer et al. [20] to the ^{111m}Cd HCA I perturbed angular correlation spectrum.

Results and Discussion

The measured K X ray coincidence and anti-coincidence perturbed angular correlation spectra for ^{111}In HCA I in 50% sucrose are shown in both Figs. 2 & 3. Figure 2 shows theoretical spectra for the chemical transmutation model at parameter values listed in Table I and Fig. 3 shows theoretical spectra for the dose dependent damage model at parameter values listed in Table II. The procedure for approximately fitting the models is given in the methods section. Relaxation in the chemical transmutation model spectra results from metastable coordination complex decay and molecular tumbling. Evidently these mechanisms can account for all relaxation experimentally observed in ^{111}In HCA I perturbed angular correlation spectra. Since the coordination complex initial metastable state is assumed to be independent of the Auger emission intensity, the chemical transmutation model predicts equality of the K X ray coincidence and anti-coincidence spectra.

Relaxation in the dose dependent damage model spectra results from ligand reorientation. The absence of molecular tumbling relaxation in this model is a matter of convenience. Additional high precision ^{111m}Cd HCAB I spectra would be required to establish the correct balance of relaxation due to internal and overall motion. The the-

TABLE I: Chemical transmutation model quadrupole interaction parameters for perturbed angular correlation spectra of HCA I.

	^{111m}Cd	^{111}In
Metastable state		
Freq. mean (s^{-1})	-	133×10^6
Freq. SD	-	50%
Asymmetry	-	0.0
Lifetime (ns)	0.0	66
Ground state		
Freq. mean (s^{-1})	95×10^6	95×10^6
Freq. SD	18%	18%
Asymmetry	0.68	0.68
Euler angles (ϕ, θ, ψ)	-	$0, \pi/2, 0$
Tumbling lifetime(ns)	81	81

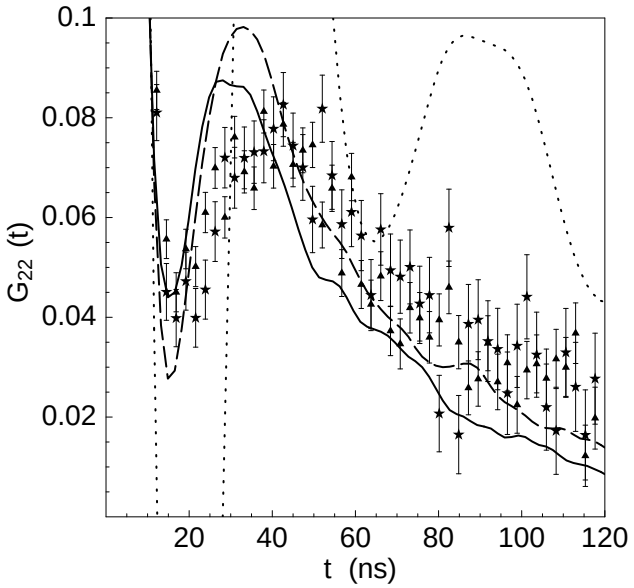

FIG. 3: Dose dependent damage model for HCA I perturbed angular correlation spectra. The experimental data is identical to that displayed in Fig. 2. The solid curve is an approximate fit of the dose dependent damage model to the data. The dotted curve is an approximate fit to the ^{111m}Cd HCA I perturbed angular correlation spectrum with relaxation from ligand reorientation rather than molecular tumbling. The dashed curve is the dose dependent damage model for the K X ray coincidence HCA I perturbed angular correlation spectrum derived by linear interpolation of the model parameters for the ^{111m}Cd and K X ray anti-coincidence spectra.

oretical K X ray coincidence and anti-coincidence spectra for the dose dependent damage model depend upon the relative Auger emission intensities. The electron capture decay of ^{111}In in coincidence with a cadmium K X ray yields on average 11.0 Auger and Coster-Kronig electrons and in anti-coincidence yields on average 16.8

TABLE II: Dose dependent damage model quadrupole interaction parameters.

	^{111m}Cd	^{111}In $(k+)$	^{111}In $(k-)$
Freq. mean (s^{-1})	95×10^6	127×10^6	133×10^6
Freq. SD	18%	47.6%	53%
Asymmetry	0.68	0.468	0.43
Rotation SD	25°	37.7°	40°
Jump lifetime (ns)	26.5	18.1	16.5

electrons (R. W. Howell, private communication). The anti-coincidence yield must be corrected for the efficiency of detection for K X rays. The corrected anti-coincidence yield,

$$Y'_{k-} = \frac{(1-\omega)}{1-\epsilon\omega} Y_{k-} + \frac{\omega(1-\epsilon)}{1-\epsilon\omega} Y_{k+}, \qquad (3)$$

where ϵ is the K X ray detection efficiency, ω is the probability per decay of K X ray emission, Y_{k-} is the perfect anti-coincidence yield, and Y_{k+} the K X ray coincidence yield. At the estimated detection efficiency for cadmium K X rays of 23%, the corrected anti-coincidence Auger electron yield is 13.0. The ratio $Y_{k+}/Y'_{k-} = 11/13$ interpolates the K X ray coincidence parameters between the zero dose and K X ray anti-coincidence parameters in the dose dependent damage model. The ratio of the difference between the K X ray coincidence and zero dose parameters to the difference between the K X ray anti-coincidence and zero dose parameters is 11/13, see Table II. The experimental ^{111}In HCA I K X ray coincidence and anti-coincidence spectra are identical. However, since the difference in the theoretical K X ray coincidence and anti-coincidence spectra is small enough relative to the experimental error, the dose dependent damage model may not be confidently rejected.

Conclusions

The indistinguishability of the experimental ^{111}In HCA I K X ray coincidence and anti-coincidence spectra suggests that during the first 10^{-8} seconds following electron capture decay the hot atom chemistry is independent of the Auger and Coster-Kronig electron emission intensity. As demonstrated by the dose dependent damage model, the experimental data do not conclusively rule out dependence of hot atom chemistry on emission intensity. The difference between the HCA I K X ray coincidence and anti-coincidence spectra could be significantly increased by detecting K_β X rays for the coincidence spectrum, increasing the detection efficiency of all K X rays for the anti-coincidence spectrum, and possibly by measuring at liquid nitrogen temperature.

Special thanks are due to Kandula S. R. Sastry and

Franklyn G. Prendergast for their continued encouragement and support of this project. Lynda McDowell purified HCA I and helped with indium binding assays. Heiner Winkler introduced me to the Monte Carlo procedure [21] for computing a perturbation factor by averaging over the probability distribution of piecewise static interactions. Roger Howell provided electron yields. Alexander Halpern has called to my attention references [1, 2, 3, 9]. This work was supported in part by National Institutes of Health grant 1 R03 RR02219-01.

* Electronic address: haydock@mailaps.org; Current address 1326 2nd St. NW, Rochester, MN 55901

[1] J. P. Adloff, Radiochim. Acta **25**, 57 (1978).
[2] P. Boyer and A. Baudry, in *Hot Atom Chemistry*, edited by T. Matsuura (Elsevier, Amsterdam, 1984), pp. 315–347.
[3] H. Sano and P. Gütlich, in *Hot Atom Chemistry*, edited by T. Matsuura (Elsevier, Amsterdam, 1984), pp. 265–302.
[4] M. Alflen, C. Hennen, F. Tuczek, H. Spiering, P. Gütlich, and Z. Kajcsos, Hyperfine Interact. **47**, 115 (1989).
[5] C. Haydock and K. S. R. Sastry, in *Proceedings of the 8th International Congress of Radiation Research* (1987), vol. 1, p. 67.
[6] T. Kobayashi, K. Fukumura, T. Kitahara, and S. Shimizu, J. Phys. Colloq. pp. C28–29 (1979).
[7] C. M. Lederer and V. S. Shirley, eds., *Table of Isotopes* (John Wiley, New York, 1978), pp. 516–523, seventh ed., A = 111, URL `http://ie.lbl.gov/toi/nucSearch.asp`.
[8] H. Kim and D. D. Dlott, J. Chem. Phys. **94**, 8203 (1991).
[9] B. Diehn, A. Halpern, and G. Stöcklin, J. Am. Chem. Soc. **98**, 1077 (1976).
[10] R. G. Khalifah, D. J. Strader, S. H. Bryant, and S. M. Gibson, Biochemistry **16**, 2241 (1977).
[11] J. B. Hunt, M.-J. Rhee, and C. B. Storm, Anal. Biochem. **79**, 614 (1977).
[12] Y. Pocker and J. T. Stone, Biochemistry **6**, 668 (1967).
[13] H. Frauenfelder and R. M. Steffen, in *Alpha-, Beta- and Gamma- Ray Spectroscopy*, edited by K. Siegbahn (North-Holland, Amsterdam, 1965), vol. 2, chap. XIXA, pp. 997–1198.
[14] E. Matthais, W. Schneider, and R. M. Steffen, Ark. Fys. **24**, 97 (1963).
[15] H. Goldstein, *Classical Mechanics* (Addison-Wesley, Massachusetts, 1980), pp. 606–610, 2nd ed., appendix B.
[16] R. Bauer, Q. Rev. Biophys. **18**, 1 (1985).
[17] B. T. Smith, J. M. Boyle, J. J. Dongarra, B. S. Garbow, Y. Ikebe, V. C. Klema, and C. B. Moler, *Matrix Eigensystem Routines - EISPACK Guide* (Springer-Verlag, Berlin, 1976), no. 6 in Lecture Notes in Computer Science, 2nd ed.
[18] F. James, Rep. Prog. Phys. **43**, 1145 (1980).
[19] M. P. Allen and D. J. Tildesley, *Computer Simulation of Liquids* (Clarendon Press, Oxford, 1989), pp. 345–351, appendix G.
[20] R. Bauer, P. Limkilde, and J. T. Johansen, Biochemistry **15**, 334 (1976).
[21] E. Gerdau, H. Winkler, B. Giese, W. Gebert, and J. Braunsfurth, Hyperfine Interact. **1**, 469 (1976).